OPEN ACCESS
International Journal of Recent Technology and Engineering (IJRTE)
ISSN: 2277-3878 (Online), Volume-7 Issue-4, September 2018

Evaluation of Thermal Performance and Thickness of Carbon Phenolic Composite Structure under Aero-Thermal Loading

Divya Sri, B. Purna Chandra Sekhar, D.V. Seshagirirao, P.V. Surendra Mohan Kumar

***Abstract**: Aerospace structures contain multilayer structures to sustain severe aerodynamic loading and heating. Hence they will be made with a carbon-epoxy internal layer(as a structural layer) whereas carbon phenolic external layer (as thermal protection layer) as a multi-layered component. Carbon-phenolic composites are meant or heat protection of the aerospace like aircraft skins, nozzles and heat shields during the aerodynamic loading conditions. In this paper, the behavior of the thermal protection system under aero-thermal load during re-entry at hypersonic speed through the earth atmosphere has been studied. Thermal performance of the carbon-phenolic components depends on the shape of the structure, velocity of the object, angle of attack and the heat flux experienced. The heat of reaction and pyrolysis process decides the structural integrity of the thermal layer. For various velocities, shapes and heat Flux conditions, the rate of ablation, surface temperature, residual thickness of the material has been evaluated. The heat of reaction and the volume of chemical species evolved under aerodynamic heating are measured by pyrolysis gas chromatography (Py-GC) and thermo-gravimetry (TG), which will be used as inputs or thermal evaluation of the structure. Modeling of the blunt body using CAD and imported to simulation software USIM to visualize different properties of the atmosphere and blunt body model.*

***Keywords:** (as a Structural Layer), (as Thermal Protection Layer) (Py-GC) and Thermo-Gravimetry (TG),*

I. INTRODUCTION

The Re-entry Vehicle Structure (RVS) configuration consists of four conical sections. Geometry Sections are constructed by tape wound Carbon Phenolic layer over the conical shell of filament wound Carbon Epoxy. carbon epoxy structure is for taking care of the structural loads. carbon phenolic to take care of thermal loads by the ablation process.

Revised Manuscript Received on 30 September 2018.
* Correspondence Author
Divya Sri*, Department of Mechanical Engineering, Achara Nagarjuna University, Guntur (A.P), India
B.purna Chandra Sekhar, Assistant professor, Department of Mechanical Engineering, Achara Nagarjuna University, Guntur (A.P), India
D.V.Seshagirirao, Assistant Professor, Department of Mechanical Engineering, Vasireddy Venkatadri Institute of Technology, Nambur (A.P), India.
P.V.Surendra Mohan Kumar, Professor, Department of Mechanical Engineering, Vasireddy Venkatadri Institute of Technology, Nambur (A.P), India.

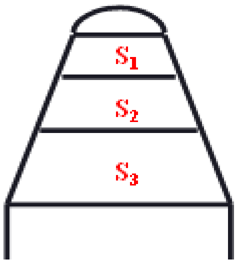

The RVS system is subjected to a severe aero-thermal environment during its flight. These thermal loads can potentially harm critical component if adequate protection is not provided. Thus the design of a suitable thermal protection system is an important part of the overall vehicle design.

II. MATERIAL PROPERTIES

The material properties of Carbon-Epoxy and Carbon Phenolic considered for analysis are listed in the table below:

Table 1: Material Properties of Carbon/Epoxy T-700 at 300K

Property	Value
E	6.0 GPa
G	4.0GPa
V	0.29

Table 2: Material Properties of Carbon/Phenolic T-700 at 300K

Property	Value
E	18.9GPa
G	4.83GPa
V	0.2

III. LITERATURE REVIEW

Yaxi Chen et al. [1] have carried out research on improved ablation resistance of carbon phenolic composites and says that the Phenol is used as a matrix and carbon is used as a reinforcement in the form of fibers in carbon phenolic composite structure. Ablation rate of the matrix is higher than the carbon fibers in C-Ph composites during the reentry. Due to aero-thermal loading a series of chemical reaction occur at the surface of the re-entry vehicle. Heating of resin releases gas as a by-product (pyrolysis gas) leaving behind char. The gas pressure in the Pyrolysis zone forces the Pyrolysis gas to flow through the *char* into the boundary layer.

L.Paglia et al. [2] by his research on Carbon-Phenolic ablative materials for re-entry space vehicles plasma wind tunnel test and finite element modeling says that due to the surface shear force and pressure gradient the surface of the blunt body is eroded. By measuring the amount of ablation and pyrolysis the effect of heat flux on the composite material can be investigated.

His-Wu Wong et al.[3] conducted detailed analysis of species production from the pyrolysis of the Phenolic Impregnated Carbon Ablator and says that due to the air flow during the Re-entry of the RVS in high dense earth atmosphere surface of the structure suffer high friction. Therefore the temperature of the surface increases. Due to this high-temperature phenol from the carbon phenolic decomposes into gases and form a protective shield around the structure this mitigate heat flux into the material.[3] By using NASA's Phenolic Impregnated Carbon Ablator (PICA), decomposition of Phenol is measured and detailed species production during pyrolysis is determined. In this review known thermodynamic data for species, it is found that a mixture of ablation gases, atmosphere air, and carbon phenolic are rich in Oxygen, Nitrogen, Carbon and Hydrogen.

James B.Scoggins et al. [4] by his research on thermodynamic properties of carbon-phenolic gas mixtures says that In the prediction of response of ablative material with atmospheric re-entry determination of species found in carbon, phenolic is very important.

Bernd Helber et al. [5] carried out research on Experimental investigation of ablation and pyrolysis of the Carbon-Phenolic ablators in atmospheric entry plasma, In this paper surface recession of ablator is studied, It is found that the surface recession is the function of the pyrolysis outgassing rate. The blunt-body surface increases up to 2800 K, The literature shows that the internal oxidation of the material did not observe during low pressure. Evaluation of the surface recession reveals after pyrolysis only low thermal conductivity char is formed and no sign of phenolic resin found.

Samire Sabagh et al. [6] carried out research on High-Temperature ablation and thermo-physical properties improvement of carbon fiber reinforced composite using graphite oxide nano-powder says that the composite structure of Carbon Phenolic have great thermal stability and ablative properties. It shows strong interfacial interaction after pyrolysis between the phenolic matrix and layered carbon structure. It is proved that the use of carbon phenolic structures gives the best result in the thermal diffusivity, thermal stability and rate of ablation with respect to other material available. This structure had constant thermal diffusivity at different temperature and improved charred formation and ablation rate during re-entry.

P.Sanoj et al. [7] in his research on Hybrid carbon-Carbon Ablative Composites for Thermal Protection in Aerospace says that the successful application of composite materials for high temperature zones in aerospace application has resulted in extensive expiation of cost effective ablative materials . High temperature heat shielding to body, be it external or internal, has become essential in the space vehicles. The heat shielding primarily protects the substrate material from external kinetic heating and the internal insulation protects the subsystems and helps to keep coefficient of thermal expansion low. Alexandre Martin et al. [8] by his results of research on chemistry model for ablating carbon-phenolic material during atmosphere re-entry, he says that A one dimensional material response implicit solver with surface ablation and pyrolysis is implicitly coupled to LeMANS, a CFD code for the simulation of weakly ionized hypersonic flows in thermo-chemical non-equilibrium. Following verification and validation of the blowing wall boundary conditions and ablation coupling, the implementation of a moving mesh algorithm in the flow solver is proposed. Bianchi et al. [9] on his research of Practical Navier-stokes Computation of Flow fields with Ablation Products Injection formulated detailed physical-mathematical model and its numerical solution for the analysis of the high temperature flow over a non-charring (graphite)ablating surface. The general boundary conditions and cannot be realistically used to simulate the flow field over ablating surface. The rarely available Navier-Stokes solvers include complete boundary conditions to realistically determine aero-thermal heating and surface ablation rates.

J.S. State et al. [10] by his research on Carbon/Phenolic Nano composites as Advanced Thermal Protection Material in Aerospace Applications says that Ablative nano composites were prepared by incorporating multi wall carbon nanotubes (MWCNT) into phenolic resin and then impregnating them into rayon based carbon fabric.

IV. MODELING AND SIMULATION

By using Trellis Pro 16.1 3D Model of Blunt body is created according to the dimensions specified. Geometry is a circular cone with base circle radius is 283.65 mm, smaller circle is 118.15mm radius and length of the cone is 938.5 mm. Model meshes with High-end Hexahedral meshing. The geometry is divided into 27140 elements. To the meshed model boundary conditions is given. [10]Carbon Phenolic material properties are assigned to the geometry. The thermal properties are;

Property	**Units**	**Value**
Density	Kg/m^3	1400
Specific Heat	J/kg-K	937.8
Conductivity	W/m-K	0.5598

The last step in the modeling is to import the mesh for analysis. USIM support only genesis format i.e. .g.USIM is used to solve, a two-dimensional axisymmetric Navier-Stokes equation. Solutions with various surface boundary conditions were obtained to study the effects on surface composition and ablation rate of the blunt body [9]. The simulation is performed at an altitude of 61 km, the speed 7650 m/s, the angle of attack is 00, free stream density is $2.816^{-4}kg/m^3$. and temperature 244.3 K respectively. [8]The fluid contains 7 air species and carbon phenolic atoms. In the external text data file air7SpeciesAbCarbon.txt in USIM, The reactions and atomic data are given.

V.RESULTS AND DISCUSSION

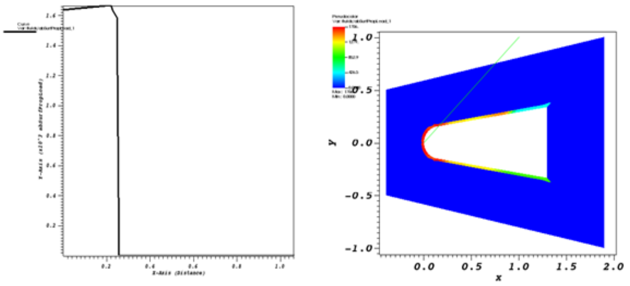

Fig 2: 1-D & 2-D Analysis of Aerodynamic load distribution from tip to the aft end

In the analysis, the maximum aerodynamic loading due to air friction at the tip during entry of the rocket in the earth atmosphere is observed as 1706 N at a re-entry speed of 7650 m/s^2. The variation of aerodynamic loading along the length of the ablative surface is shown in the fig.2

Table. 4: Gradient Temperature at Various Locations.

Distance(m)	0.0	0.05	0.075	0.1	0.2	0.5	1.0
Temperature (Max) x 10^3 K	90	60	60	30	24	10	0
Temperature (Min) x 10^3 K	-175	-132	-100	-60	-41	-16.5	-42

Gradient temperature at a different location is observed from the simulation and plotted in table.4. This is the temperature between surface temperature and atmospheric plasma state temperature.

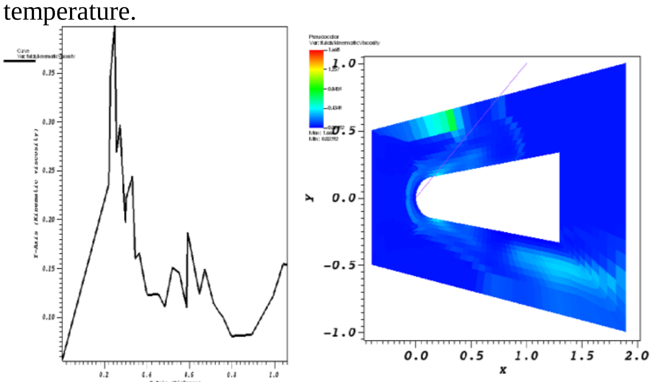

Fig 3: 1-D & 2-D Analysis of kinematic viscosity distribution from tip to the aft end

In fig. 3. The X-axis is the length of the blunt body and Y-axis is the Kinematic viscosity. The kinematic viscosity depends on the dynamic viscosity and density. The relation is

$$\vartheta = \frac{\mu}{\rho}$$

Where ϑ is the kinematic viscosity,μ is dynamic viscosity and ρ is the density.

As kinematic viscosity increases, the rate of ablation decreases.

The maximum and minimum Kinematic Viscosity is 1.668 m^2/s and 0.02392 m^2/s respectively. Variation of kinematic viscosity along ablative surface can be observed from the graph.

Table 5: Molecular weight Average at Different Stations

Distance(m)	0.0	0.05	0.075	0.1	0.2	0.5	1.0
Mw(Avg) (Max) (kg)	28.8	28.8	28.8	28.8	28.8	28.8	28.53
Mw(Avg) (Min) (kg)	18	18.6	18.6	19.4	18.9	22.35	28.82

The X-axis is the length of the blunt body and Y-axis is the Molecular weight average. Molecular weight average is found maximum at 0.0m. As the molecular weight increases, the pores size increases on the surface area creating an increase in ablation rate. Initially, the molecular weight is less so the ablation rate is also less.

The Maximum and minimum molecular weights are 28.8 kg and 17.96 kg respectively. The variation on molecular weight along the ablative surface can be observed from the graph.

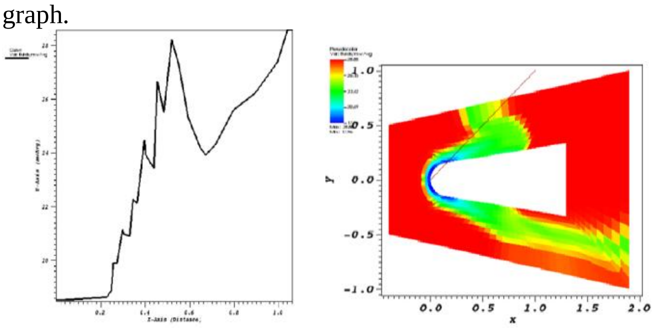

Fig 4: 1-D & 2-D Analysis of molecular weight distribution from tip to the aft end

In fig. 4. X-axis is the length of the blunt body and Y-axis is the Electron pressure. Electron pressure variation can be observed from the figure above. The maximum value of electron pressure is 15.92 N/m^2 and the minimum value is 1.255 x $10^{-011} N/m^2$. Initially, electron pressure is maximum then fall linearly becoming constant along the length of the blunt body.

Table 6: Thermal Coefficient at Different Stations

Distance (m)	0.0	0.05	0.075	0.1	0.2	0.5	1.0
Thermal Coefficient (Max) W/mk	0.25	0.24	0.235	0.235	0.235	0.177	24.58 x 10^{-3}
Thermal Coefficient (Min) W/mk	0.047	0.047	0.047	0.047	0.047	0.139	21.15 x 10^{-3}

Variation of the thermal coefficient at a different location is plotted in table .6. This effect the heat transfer rate through the body. It is observed that from tip to aft thermal coefficient is slightly changing.

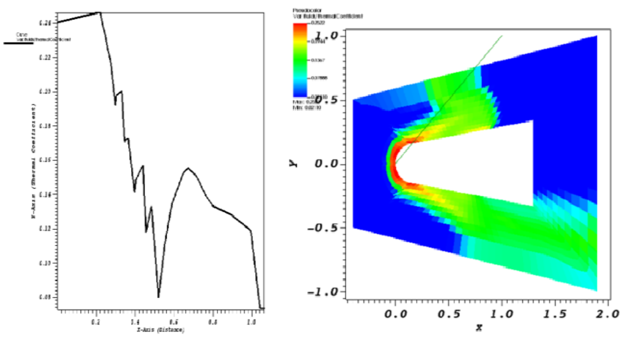

Fig 5: 1-D & 2-D Analysis of Thermal coefficient distribution from tip to the aft end

In fig. 5. X-axis is the length of the blunt body and Y-axis is the Thermal Coefficient. The thermal coefficient of carbon phenolic depends on the corresponding temperature of the wall, T=300K. As the wall temperature increases the heat flux rate drops. The maximum value of the thermal coefficient obtained is 0.2522 W/mk. the minimum value obtained is 0.0211 W/mK.

The variation of thermal coefficient along the surface of the blunt body can be observed in the graph

Table 7: Thermal Diffusivity at Different Stations.

Distance(m)	0.0	0.05	0.075	0.1	0.2	0.5	1.0
Thermal Diffusivity (Max)	0.44	0.44	0.56	0.56	0.72	0.292	0.0864
Thermal Diffusivity (Min)	0.057	0.057	0.08	0.08	0.08	0.118	0.075

Thermal diffusivity shows the capacity of the body to absorb heat. Its value at a different station is plotted in table .7.

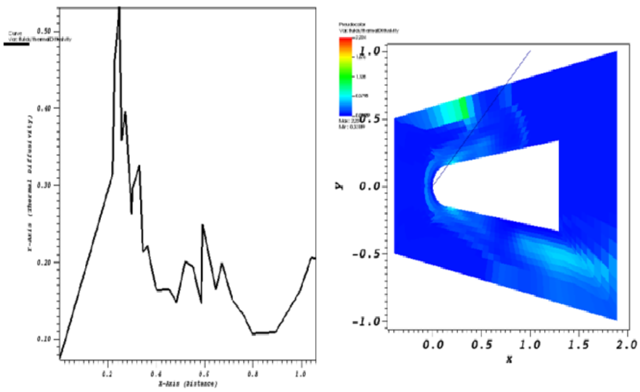

Fig 6: 1-D & 2-D Analysis of Thermal diffusivity distribution from tip to the aft end

In fig. 6. X-axis is the length of the blunt body and Y-axis is the Thermal Diffusivity. Thermal diffusivity depends on the thermal conductivity of carbon phenolic. As thermal conductivity of carbon phenolic decreases, the thermal diffusibility also decreases thus heat conduction would be less. Here from the graph, it is found that the maximum value of thermal diffusivity is 2.22 and the minimum value obtained is 0.0318

Table 8: Viscous Source at Different Stations.

Distance(m)	0.0	0.05	0.075	0.1	0.2	0.5	1.0
Viscous Source (Max)	754	550	660	320	340	114	49
Viscous Source (Min)	-180	-260	-440	-440	-260	-60	2.0

Variation of the viscous source at a different location along the length of the blunt body is plotted in table.8.

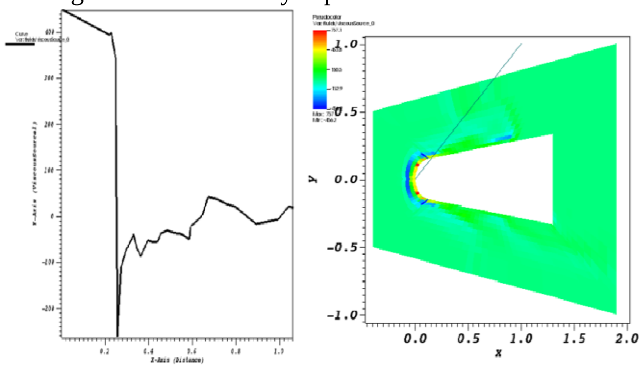

Fig 7: 1-D & 2-D Analysis of Viscous source distribution from tip to the aft end

In fig. 7 X-axis is the length of the blunt body and Y-axis is the Viscous source 1. This figure illustrates the viscous source of a re-entry vehicle, the maximum obtained is 757.1Ns/m which is plotted along Y-axis and the minimum value obtained is -456.2 Ns/m which is plotted along negative Y-axis of the graph. The variation of viscous along the surface of the blunt body can be observed from the graph.

As the viscosity of surrounding gas increases due to increase in temperature i.e. rate of heat increases, thus ablation rate also increases.

Different parameters were visualized from 3D re-entry simulation carried out by USIM. It is observed that chemical reaction and temperature of the surrounding atmosphere is so massive that the surface temperature of the blunt body increases. The surface temperature at the tip is 3.3×10^3 K and at the aft, 264 K is observed. Further, this temperature will help for the analysis of carbon phenolic ablation rate and effect of temperature on the durability of the structure.

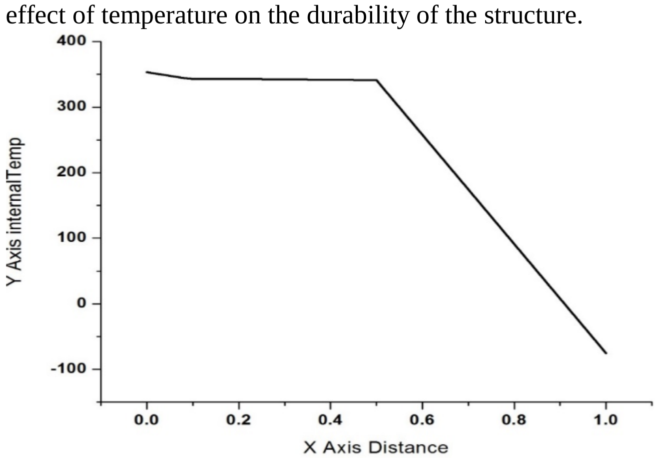

Fig 8: Internal Temperature of RVS

The internal temperature of RVS is to be maintained at 80^0C for the sustainability of the internal structure. This temperature limit can be achieved from the above fig.8. It is observed that the internal temperature is maximum at nose slightly changing up to 0.5 m length of the RVS and then fall linearly at the aft.

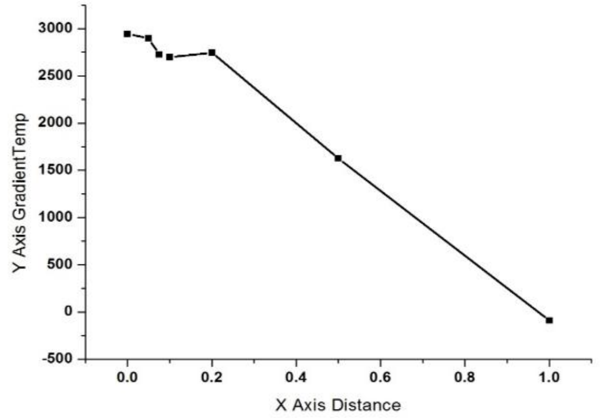

Fig 9: Gradient temp Vs Distance

Variation of gradient temperature along the length of the blunt body can be observed from the fig. 9. At the nose maximum temperature is 2947 K and at the aft end, i.e at 1 meter distance is -89 K.

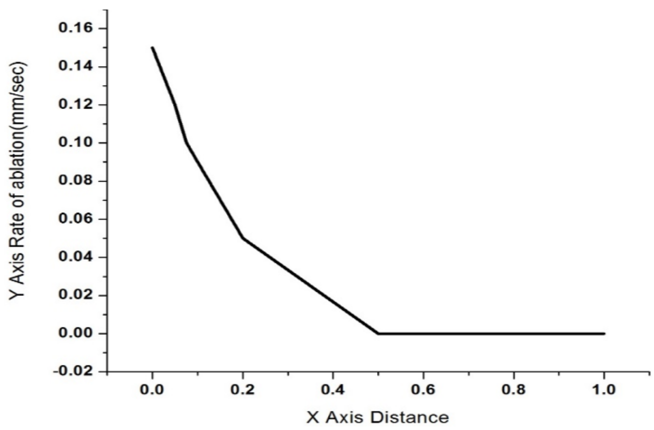

Fig. 10: Rate of ablation Vs Distance

During re-entry, atmospheric drag slows the RV, and the kinetic energy of the RV is converted into thermal energy of the air, producing a layer of extremely hot air surrounding the RV. A small fraction of this heat is then transferred to the RV body: our calculations show that for RVS with low weight-to-drag ratios roughly 1-2 percent of the total re-entry heat will be transferred to the RV, while for modern RVS with high weight-to-drag ratios ($\beta \approx$ 120,000 N/m2), 6-10 percent of the total re-entry heat will be transferred for both minimum-energy and depressed trajectories. However, the total heat transferred to the RV is significant because the kinetic energy change of strategic RVs is extremely large (~10^9 joules).

The variation of ablation rate during the re-entry of the RV can be observed from figure 10.It is observed that at nose maximum ablation is 0.15 mm/sec this ablation fall along the length of the RV at 0.5 m the ablation rate is constant. The reference thickness of carbon phenolic shell is 9 mm. From the figure it is observed that the maximum ablation rate is 0.1-0.15 mm/s for re-entry duration of 30 seconds. The total thickness ablated in 30 seconds is calculated as 4.5 mm. considering the structural safety factor; the total thickness is calculated to be 7.5 mm. Therefore through the above analysis, the optimization of thickness is 1.5 mm. From this thickness, it is found that the weight of material has reduced compared to earlier design weight. This reduction in weight increases the performance of the vehicle in terms of weight and range.

VI. CONCLUSIONS

- The heat of reaction and nature of Pyrolysis gases evaluated using gas chromatography.
- The surface temperature, heat flux, and heat penetration through the thickness are visualized using USIM software.
- The heat of Pyrolysis was determined from measured differential thermal analysis data.
- In the present tests, mechanical char removal did occur at certain test conditions depending on the mass fraction of oxygen in the stream and the stagnation pressure.
- The mechanical char removal did occur for tests in air at pressures above 2.4 atmospheres and air-nitrogen mixtures above 6 atmospheres.
- The mechanical char removal occurred at the surface of the char and did not remove the entire char layer.

REFERENCES

1. Yaxi Chen, Ping Chen, Changqing Hong, Baoxi Zhang, David Hui 2013 Improved ablation resistance of carbon–phenolic composites by introducing zirconium diboride particles *J. Composites Part B: Engineering*. 47 320-325.
2. L.Paglia, J.Tirillò, F.Marra, C.Bartuli, A.Simone, T.Valente, G.Pulci 2016 Carbon-phenolic ablative materials for re-entry space vehicles: plasma wind tunnel test and finite element modeling *J. Materials & Design*. 90 1170-1180.
3. Hsi-Wu Wong, Jay Peck, James Assif, Francesco Panerai, Jean Lachaud, Nagi N.Mansour 2016 Detailed analysis of species production from the pyrolysis of the Phenolic Impregnated Carbon Ablator *J. Journal of Analytical and Applied Pyrolysis* 122. 258-267.
4. James B.Scoggins, Jason Rabinovitch, Benjamin Barros-Fernandez, Alexandre Martin, Jean Lachaud, Richard L.Jaffe, Nagi N.Mansour, Guillaume Blanquart, Thierry E.Magin 2017 Thermodynamic properties of carbon–phenolic gas mixtures *J. Aerospace Science and Technology*. 66 177-192.
5. Bernd Helber, Alessandro Turchi, James B.Scoggins, Annick Hubin, Thierry E.Magin 2016 Experimental investigation of ablation and pyrolysis processes of carbon-phenolic ablators in atmospheric entry plasmas *J.* International Journal of Heat and Mass Transfer. 100 810-824.
6. Samire Sabagh, Ahmad Aref Azar, Ahmad Reza Bahramian 2017 High-temperature ablation and thermo-physical properties improvement of carbon fiber reinforced composite using graphene oxide nanopowder *J. Composites Part A: Applied Science and Manufacturing* 101. 326-333.
7. P. Sanoj, Balasubramanian Kandasubramanian 2014 Hybrid Carbon-Carbon Ablative Composites for Thermal Protection in Aerospace *J. Journal of Composites* 825607. 15.
8. Alexandre Martin, Iain D. Boyd 2010 Chemistry model for ablating carbon-phenolic material during atmospheric re-entry J. AIAA 2010-1175.
9. Bianchi, D, Martelli, E, Onofri, M 2006 Practical Navier-Stokes Computation of Flowfields with Ablation Products Injection *J. Thermal Protection Systems and Hot Structures* 631. 15.
10. J. S. Tate, S. Gaikwad, N. Theodoropoulou, E. Trevino, J. H. Koo 2013 Carbon/Phenolic Nanocomposites as Advanced Thermal Protection Material in Aerospace Applications *J. Journal of Composites* ID 403656. 9.